The Journal of Neuroscience, January 15, 2002, 22(2):437–445

Multipotent Neural Stem Cells Reside into the Rostral Extension and Olfactory Bulb of Adult Rodents

Angela Gritti,[1] Luca Bonfanti,[2] Fiona Doetsch,[3] Isabelle Caille,[3] Arturo Alvarez-Buylla,[3] Daniel A. Lim,[3] Rossella Galli,[1] Jose Manuel Garcia Verdugo,[4] Daniel G. Herrera,[1] and Angelo L. Vescovi[1]

[1]Institute for Stem Cell Research, Department of Biotechnology, San Raffaele Hospital, 20132 Milan, Italy, [2]Department of Morphophysiology, University of Turin, 10100 Turin, Italy, [3]The Rockefeller University, New York, New York 10021, and [4]University of Valencia, Burjasot, 46100 Spain

The lateral walls of the forebrain lateral ventricles are the richest source of stem cells in the adult mammalian brain. These stem cells give rise to new olfactory neurons that are renewed throughout life. The neurons originate in the subventricular zone (SVZ), migrate within the rostral extension (RE) of the SVZ along the rostral migratory stream (RMS) within tube-like structures formed of glial cells, to eventually reach the olfactory bulb (OB). We demonstrate that, contrary to the current view, multipotential (neuronal–astroglial–oligodendroglial) precursors with stem cell features can be isolated not only from the SVZ but also from the entire RE, including the distal portion within the OB. Specifically, these stem cells do not derive from the migratory neuroblasts coming from the SVZ. Interestingly, stem cells isolated from the proximal RE generate significantly more oligodendrocytes, and those from the distal RE proliferate significantly more slowly than stem cells derived from the SVZ and other RE regions. These findings demonstrate that stem cells are not confined to the forebrain periventricular region and indicate that stem cells endowed with different functional characteristics occur at different levels of the SVZ–RE pathway.

Key words: adult neural stem cells; multipotent precursors; forebrain subventricular region; rostral extension; olfactory bulb; neurogenesis

Multipotential neural stem cells can be isolated from the forebrain periventricular region of the adult mammalian brain (Reynolds and Weiss, 1992; Richards et al., 1992; Morshead et al., 1994; Gritti et al., 1996; Temple and Alvarez-Buylla, 1999; Doetsch et al., 1999a, Johansson et al., 1999). The subventricular zone (SVZ) lines most of the lateral wall of the lateral ventricles in adult rodents. Although *in vitro* forebrain periventricular stem cells display multipotency (for review, see Weiss et al., 1996; McKay, 1997; Temple and Alvarez Buylla, 1999; Gage, 2000), *in vivo* SVZ precursors generate primarily committed neuronal precursors that migrate tangentially along the rostral extension (RE) of the SVZ toward the olfactory bulb (OB), constituting the rostral migratory stream (RMS). Within the RMS these neuroblasts (type A cells) form elongated aggregates called chains and continue to divide while migrating (Menezes et al., 1995; Wichterle et al., 1997) through glial tunnels formed by the processes of astrocytes (type B cells; Lois et al., 1996). After reaching the core of the OB they move radially into the granular and periglomerular layers, where they differentiate into mature neurons (Luskin, 1993; Lois and Alvarez-Buylla, 1994). These findings gave rise to the current view that the forebrain periventricular region is a stem cell reservoir, and the RE is a conduit for the neuronal progeny of these cells that are targeted to more rostral brain regions. This view renders the idea that the RE itself could be a primary source of multipotential stem cells rather counterintuitive. However, it has been observed that the ratio of proliferating to nonproliferating cells along the RMS considerably exceeds the ratio of proliferating to nonproliferating lateral ventricle-derived cells that are migrating along the RMS (Menezes et al., 1995; Craig et al., 1999), suggesting that some of the mitotically active precursors within the RMS may be generated *in situ*. We therefore investigated whether multipotential stem cells are present in the RE. In the present work we show that stem cells can be cultured from all parts of the RE, including the region within the OB. Cells isolated from different levels of the RE proliferate *in vitro*, as determined by neural stem cell colony-forming assay (Stemple and Anderson, 1992; Gritti et al., 1996, 1999), and display extensive self-renewal properties and multipotentiality in long-term cultures. These stem cells show growth profiles and differentiation potentials that are similar, but not identical, to those of their periventricular counterparts. Importantly, we show that they reside within the RE itself and do not migrate into the RE from the SVZ.

MATERIALS AND METHODS

Primary cultures

Three-month-old or postnatal day 15 (P15) CD-1 albino mice (Charles River) were anesthetized by intraperitoneal injection of 4% chloral hydrate (0.1 ml/10 gm body weight) and killed by decapitation. The brains were removed from adult mice and tissues containing the SVZ, and the RE1 and the RE2 were dissected out (see Results) (Fig. 1). Tissues derived from two mice were pooled to generate each culture. In some experiments the RE of the OB was isolated, taking care not to include the surrounding parenchyma, which was cultured as a separate sample (Fig. 1). In some experiments the optic nerve, the cerebral cortex, and the OB were isolated separately, taking care not to include tissue from the RE. The optic nerve was also isolated from P15 animals. In a

Received July 10, 2001; revised Oct. 5, 2001; accepted Oct. 25, 2001.

This work was supported by Italian Telethon Grant 1246 and European Community grants to A.L.V. We thank Drs. H. Witcherlie and Dr. Daniela Ferrari for technical help in the dissection procedure and immunofluorescence analysis, D. Ward for critical review of the English, and G. Calori for the statistical analysis.

Correspondence should be addressed to Angela Gritti or Angelo Vescovi, Institute for Stem Cell Research, Department of Biotechnology, San Raffaele Hospital, Via Olgettina 58, 20132 Milan, Italy. E-mail: vescovi.angelo@hsr.it or gritti.angela@hsr.it.

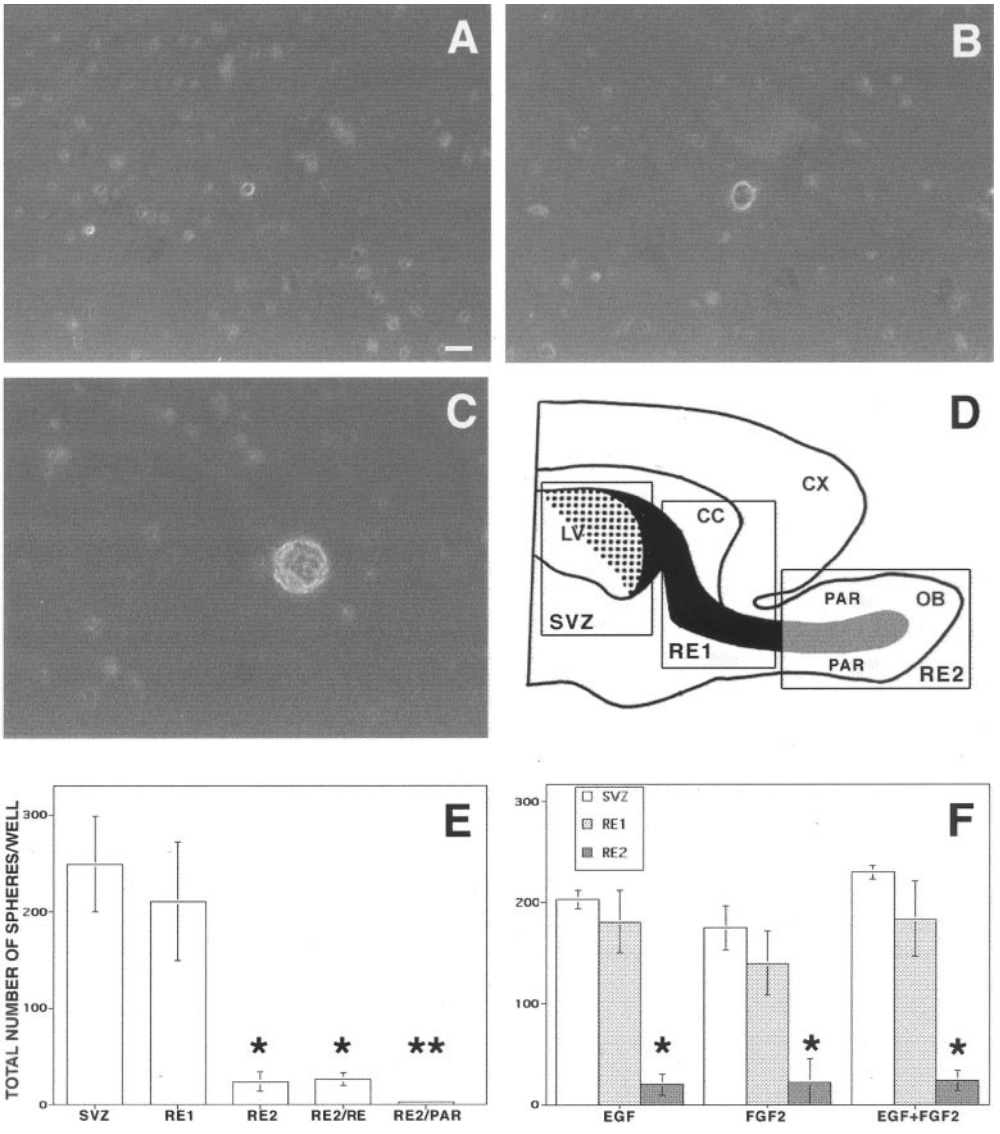

Figure 1. Undifferentiated cells isolated from the RE of adult mice proliferate in response to GFs. The forebrain of adult mice was dissected out, and three different regions were isolated (*D*): *SVZ*, subventricular zone; *RE1*, rostral extension in olfactory peduncle; *RE2*, rostral extension in the OB. SVZ–RE tissue is indicated in *black* (the *dotted area* shows the ventricular wall); RE tissue of the OB obtained by microdissection (not including the surrounding parenchyma) is indicated in *gray*. *LV*, Lateral ventricle; *CX*, cortex; *CC*, corpus callosum; *PAR*, parenchyma. Cells were cultured in the presence of EGF, FGF-2, or both; the number of spheres formed in each well was counted after 7–12 DIV. *A,* Hypertrophic cell from RE2 after 4 DIV proliferates and gives rise after 8 DIV to a small cluster of proliferating cells (*B*). After 12 DIV a primary sphere is formed (*C*). *E,* Spheres were generated from cells isolated from all three regions, but significantly fewer were obtained from RE2-derived cultures compared with those derived from SVZ and RE1. Microdissection and separation of the RE2 region into RE tissue (*RE2/RE*) and surrounding parenchyma (*RE2/PAR*), followed by culturing, showed that only cells dissociated from RE2/RE gave rise to spheres. *F,* Use of EGF, FGF-2, or both generated closely similar numbers of spheres in each of the three regions. Data are means ± SD of four independent experiments in triplicate. Tissue from two mice was pooled in each experiment. Scale bar, 20 μm. *Significantly different from SVZ and RE1; **significantly different from RE2/RE; Student's t test, $p < 0.05$.

group of adult animals unilateral olfactory bulbectomy was performed, and the tissue was processed as a separate sample. Dissected tissue from each region was transferred to Earl's Balanced Salt Solution (Invitrogen, San Diego, CA) containing 1 mg/ml papain (27 U/mg; Sigma, St. Louis, MO), 0.2 mg/ml cysteine (Sigma), and 0.2 mg/ml EDTA (Sigma) and incubated for 45 min at 37°C on a rocking platform. Tissues were then transferred to DMEM–F-12 medium (1/1 v/v; Invitrogen) containing 0.7 mg/ml ovomucoid (Sigma) and mechanically dissociated. Cells were resuspended in growth factor (GF)-free, chemically defined DMEM–F-12 medium (control medium) (Gritti et al., 1996).

Culture propagation, population analysis, and cloning

Primary cells isolated as above were plated in 35 mm plastic Petri dishes (200 cells/cm^2) in control medium containing 20 ng/ml of either epidermal growth factor (EGF) or fibroblast growth factor (FGF-2) or both (Peprotech, Rocky Hill, NY) (growth medium). The number of primary spheres was counted after 7–12 d *in vitro* (DIV). To assess for self-renewal, individual primary spheres were mechanically dissociated, and single cells were plated in growth medium; the number of secondary spheres generated from each primary sphere was counted after 7–12 d. To assess for multipotentiality, individual primary spheres were transferred onto matrigel-coated glass coverslips (12 mm diameter) in the presence of 20 ng/ml of FGF-2. After 48 hr cultures were shifted to control containing 2% fetal bovine serum (FBS) (Invitrogen) (differentiating medium). Either 1 hr or 6 d after plating cultures were fixed in 4% paraformaldehyde and processed for triple-label immunocytochemistry (see below).

For population analysis, primary spheres were mechanically dissociated to a single cell suspension and replated in growth medium (3500 cells/cm^2). This procedure was repeated twice; bulk cultures were then generated by replating cells in growth medium at a density of 10^4 cells/cm^2. The number of viable cells was assessed at each passage by Trypan blue exclusion. For growth curves, 250,000 viable cells were initially plated in a 25 cm^2 flask (0 DIV). At each subculture passage (every 4–6 d) the total number of viable cells was counted, and 250,000 cells were replated under the same conditions. This procedure was repeated for at least five subculture passages. The estimated total number of cells was calculated by multiplying the amplification rate (total number of cells obtained at a given subculture passage/250,000) for the total number of cells obtained at the previous passage. To assess maintenance of multipotentiality, an aliquot of cells was withdrawn from cell cultures at progressive subculturing steps; the cells were then differentiated and processed for immunocytochemistry (see below).

For clonal analysis single cells were transferred by micromanipulation to each well of a 96-well plate (1 cell/well) in growth medium. Individual primary clones were either differentiated to assess multipotentiality (see below) or used to establish a clonal cell line. In the latter case, they were mechanically dissociated, and individual cells were replated under the same culture conditions. The secondary clones obtained were pooled, mechanically dissociated to a single cell suspension, and replated in growth medium to establish a bulk culture.

The composition of the culture media used in different experimental conditions is summarized below.

Table 1. The functional and immunocytochemical characteristics of the different cell types in the SVZ–RE system of adult mice

Features	Type A (neuroblasts)	Type B (astrocytes)	Type C (precursors)
Proliferation rate	Fast	Slow	Fast
Migration	Yes	No	No
Tuj1-IR	Yes	No	No
PSA-NCAM-IR	Yes	No	No
GFAP-IR	No	Yes	No
Nestin-IR	Yes	Yes	Yes

Control medium. DMEM–F-12 medium (1/1 v/v) containing L-glutamine (2 mM), glucose (0.6%), putrescine (9.6 μg/ml), insulin (0.025 mg/ml), progesterone (6.3 ng/ml), apo-transferrin (0.1 mg/ml), and sodium selenite (5.2 ng/ml). This is the basal medium used to prepare the experimental media (growth and differentiation media).

Growth medium. Control medium containing mitogens (EGF, 20 ng/ml; FGF-2, 10 ng/ml). This is the medium used to isolate, grow, and expand stem cells.

Differentiating medium. Control medium containing 2% FBS. This is the medium used to generate differentiated cultures on which a quantitative analysis of the different cell types (neurons, astrocytes, and oligodendrocytes) was performed.

Ara-C cytotoxicity experiments

Ara-C (2%; Sigma) in 0.9% saline or saline alone was infused onto the surface of the brain of adult CD-1 male mice (3 months) with a minio-smotic pump (model 1007D; Alzet, Palo Alto, CA; flow rate, 0.5 μl/hr). Cannulas were implanted onto the surface of the brain at anteroposterior 0, lateral 1.1 mm relative to bregma. After 6 d of infusion mice were killed immediately or at the indicated survivals after pump removal (n = 3 for each survival time point); the brains were removed, and RE tissue was dissected out and processed for the neurosphere-forming assay (see above) or for EM analysis (see below).

Fractionation experiments

Freshly dissociated RE cells were fractionated by differential adhesion to poly-D-lysine-treated (Sigma) plastic substrates as previously described (Lim and Alvarez-Buylla, 1999). Briefly, fraction 1 (highly enriched for type A cells) was collected by washing the nonadherent cells off the plate. Fraction 4 (enriched in "type B/C" cells) was collected by trypsinization, after exhaustive washing of nonadherent cells. The cell fractions were plated either for the neurosphere-forming assay or in differentiating conditions to detect neuronal and glial antigens by immunofluorescence assay (see below).

The functional and immunocytochemical characteristics of the different cell types in the SVZ–RE system of adult mice are summarized in Table 1.

Immunocytochemistry

Double- and triple-labeling immunofluorescence was performed as previously described (Gritti et al., 1996, 1999). Briefly, cultures were fixed for 20 min in PBS containing 4% paraformaldehyde, alone or with 1% glutaraldehyde, pH 7.4, then rinsed with PBS and incubated for 90 min at 37°C in PBS containing 10% normal goat serum (NGS), 0.3% Triton X-100, and appropriate primary antibodies or antisera. After washing, cells were reacted for 1 hr at room temperature (RT) with the appropriate secondary antibodies. Samples were rinsed three times with PBS, once with distilled water, and mounted with Fluorsave (Calbiochem, La Jolla, CA).

For triple-labeling immunofluorescence, cells were permeabilized for 5 min at RT in PBS–10% NGS–0.1%Triton X-100 and incubated in a solution containing anti-microtubule-associated protein 2 (MAP-2) or anti β-tubulin type III and anti-glial fibrillary acidic protein(GFAP) antibodies in PBS and 10% NGS. Cells were then reacted with anti-mouse Alexa 488-conjugated and anti-rabbit 7-amino-4-methylcoumarin-3-acetic acid (AMCA)-conjugated secondary antibodies. After thorough washing, cells were incubated with anti-O4, followed by donkey anti-mouse IgM Cy3-conjugated secondary antibody.

Primary antibodies and antisera used: mouse monoclonal anti-MAP-2 (IgG, 1:200; Boehringer Mannheim, Indianapolis, IN), anti-β-tubulin type III (Tuj1; IgG, 1:250; Covance), anti-galactocerebroside C (GalC; IgG, 1:50; Chemicon, Temecula, CA), and anti-O4 (IgM, 1:25; Chemicon); rabbit antisera against GFAP (1:200; Dako, Carpinteria, CA), GABA (1:3000; Sigma), choline acetyltransferase (ChAT; 1:400, Chemicon), glutamic acid (1:3000; Sigma) and tyrosine hydroxylase (TH; 1:200, Protos Biotech Corporation). Secondary antibodies used: goat anti-mouse or anti-rabbit IgG antibodies conjugated with the cyanine dye Cy3 (1:1000; Jackson ImmunoResearch, West Grove, PA), with AMCA (1:100; Jackson ImmunoResearch) or with Alexa 488 (1:500; Molecular Probes, Eugene, OR); Cy3-conjugated donkey anti-mouse IgM antibody (1:100; Jackson ImmunoResearch). Samples were examined and photographed using a Nikon Eclipse 3000 fluorescence microscope. No labeling was observed in the absence of primary antibodies and antisera (control samples), and no evidence of cross-reactivity was observed. The number of cells immunoreactive (IR) for different antigens was counted in at least eight nonoverlapping fields in each sample, for a total of >500 cells per sample. The total number of cells in each field was determined by counterstaining cell nuclei with 4,6-diamidine-2-phenylindole dihydrochloride (DAPI; Sigma; 50 μg/ml in PBS for 15 min at RT).

Electron microscopy

Brains were processed for EM as described (Doetsch et al., 1997, 1999). Briefly, adult mice were anesthetized deeply with Nembutal and perfused transcardially with 0.9% saline, followed by 100 ml of Karnowsky's fixative (2% paraformaldehyde and 2.5% glutaraldehyde). Heads were removed and post-fixed in the same fixative overnight. The brains were removed and washed in 0.1 M phosphate buffer for 2 hr. The REs of control and Ara-C-treated mice were serially sectioned and analyzed at the electron microscope. Two hundred serial 70 nm ultrathin sections were obtained from one mouse, each for every time point after pump removal. The number of different cell types in the entire rostrocaudal extent of the RE was determined at the EM in two ultrathin sections for each animal (n = 3 for each time point). Cells with only small fragments of cytoplasm or nucleus in a given section were classified as unidentified. Total cell counts obtained by single-section analysis are comparable with those in three-dimensional reconstructions, indicating that the cell counts are not biased by cell size (Doetsch et al., 1997).

RESULTS

The RE of the adult brain contains multipotent undifferentiated progenitors that proliferate in response to GFs

We began our study by quantifying the number of stem cells that could be isolated from different regions of the SVZ–RE of adult mice. Brain tissue was dissected out from three levels of this pathway: (1) the forebrain periventricular region (SVZ), (2) the tract between the lateral ventricles and the OB (RE1), and (3) the OB (RE2) (Fig. 1*D*). Tissues obtained from unilateral olfactory bulbectomy performed on anesthetized animals (allowed to recover) were also included as additional, separate samples. Tissues were dissociated, and the same number of cells from each region was cultured according to a culture protocol in which the number of cell clusters generated in each well (Fig. 1*A–C, spheres*) represents the number of stem cells plated in the dish (neurosphere-forming assay; Morshead et al., 1994; Gritti et al., 1996, 1999). We found that 252.8 ± 60.4, 235.4 ± 43.7, and 23.6 ± 9.9 spheres per well were generated in SVZ-, RE1-, and RE2-derived cultures, respectively (Fig. 1*E*). As shown previously for SVZ cultures (Gritti et al., 1999), this result did not significantly change when EGF or FGF-2 were used as mitogens, either alone or in combination (Fig. 1*F*). No spheres were ever observed in cultures deriving from either the cerebral cortex or the optic nerve (both from P15 and adult mice). Moreover, when OB tissue was carefully microdissected into RE-containing and RE-devoid samples (Fig. 1*D*), sphere formation was observed exclusively in the former (Fig. 1*E*), showing that the RE was the source of clone-forming cells.

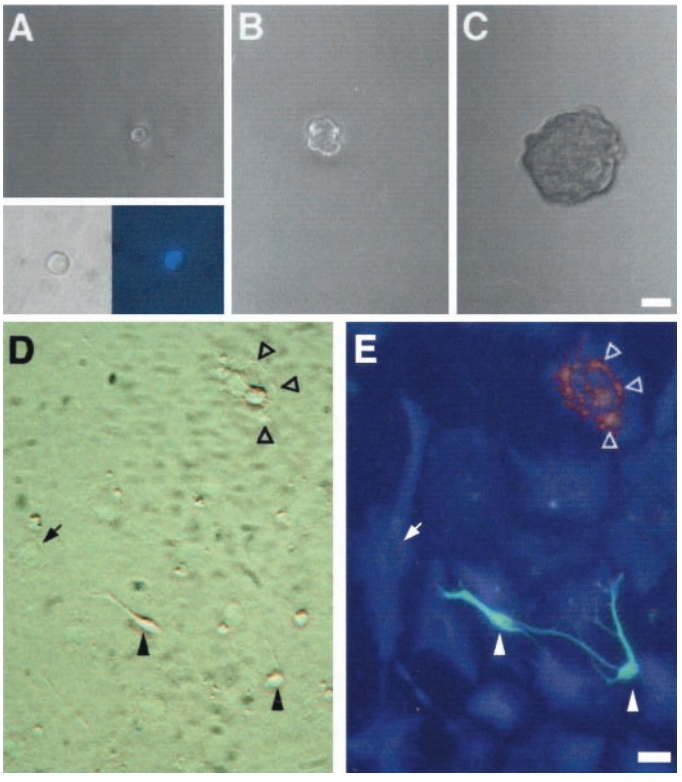

Figure 2. Cells isolated from the RE of adult mice are multipotent. Primary RE-generated spheres were dissociated, single cells were transferred to individual wells by micromanipulation (1 cell per well) in growth medium, and followed by time-lapse microphotography. Virtually all of the cells that were classified as single cells by visual inspection in our clonal assays were indeed single cells, as confirmed by the detection of a single nucleus by DAPI staining (*A, inset*). The cell shown in *A* (2 hr after plating; derived from an RE2-primary sphere) proliferated (*B*; 7 d) and gave rise after 20 d to a spherical clone of cells (primary clonal sphere; *C*). Primary clonal spheres were subcloned to generate secondary clonal spheres, which were pooled and serially passaged to generate a clonal cell line. After differentiation by removal of GFs, the progeny of RE-derived clonal cell lines included neuronal, astroglial, and oligodendroglial cells. *D, E,* Phase-contrast and fluorescence micrographs of differentiated cultures from the RE2-derived clonal cell line A7.16. Triple-labeling immunofluorescence revealed the simultaneous presence of neurons (Tuj1, *green*; *filled arrowheads*), astrocytes (GFAP, *blue*; *arrows*), and oligodendrocytes (O4, *red*; *open arrowheads*) within the same culture. Scale bars: *A–C*, 30 μm; *D*, *E*, 20 μm.

Self renewal and multipotency of RE-derived precursor cells: clonal analysis

Although cells in primary spheres derived from the SVZ, RE1, and RE2 were IR for the neuroepithelial marker nestin (data not shown), removal of mitogens resulted in their differentiation into neurons, astrocytes, and oligodendrocytes, and all three lineages occurred within each individual sphere. This indicated that the RE-derived cells might be multipotent stem cells; we therefore sought unequivocal evidence for multipotency by formal clonal analysis. Individual RE1 and RE2 cells were plated (1 cell per well) in growth medium; a subset of these cells (~2%) proliferated and gave rise to clonal primary spheres by 12–15 d (Fig. 2*A–C*), which were subcloned to generate secondary spheres. These were pooled and serially subcultured and expanded to generate bulk cultures. Two clonal cell lines were established from the RE1 (B5.14 and G4.15) and two from the RE2 (F5.14 and A7.16). Because the growth and differentiation characteristics of the clonal cell lines thus established were indistinguishable, only data from B5.14 and A7.16 are presented in the remainder of this work.

After each subculturing step, cells from clonal lines were differentiated to assess multipotency. The progeny of both cell lines always generated neurons, astrocytes, and oligodendrocytes (Fig. 2*D,E*). This confirmed that the founder cells that had given rise to each clonal line were multipotent. Importantly, the percentages of MAP-2-, GFAP-, GalC-, and O4-IR cells found in B5.14- and A7.16-derived cultures were closely similar to those found in population (bulk) studies with RE1- and RE2-derived cell lines (Table 2).

In addition to this steady differentiation potential, the RE-derived clonal lines had a stable rate of expansion over time (Fig. 3*C*). Such functional features are critical attributes of cultured stem cells and are thought to be a direct consequence of their ability to self-renew (Loeffler and Potten, 1997). To provide conclusive evidence for this ability, we used a serial subcloning approach. Cells were dissociated from primary spheres and replated as single cells in growth medium. A subset of these cells (<5%) proliferated, giving rise to secondary spheres (69.7 ± 7.6, 32.5 ± 17.0, and 55.7 ± 26.7 secondary spheres were generated from each SVZ-, RE1-, and RE2-derived primary spheres, respectively; four to eight primary spheres were analyzed for each region in two independent experiments; mean ± SD). Indirect immunofluorescence performed on individual SVZ-, RE1-, and RE2-derived primary and secondary spheres, which were triggered to differentiate by mitogen removal, revealed the presence of GFAP-, MAP-2-, and O4-IR cells (data not shown). This indicates that the primary multipotent stem cells possessed self-renewal capacity (Gritti et al., 1996, 1999; Morrison et al., 1997).

In conclusion, the entire RE, including the region inside the OB, contains undifferentiated multipotent precursors that proliferate in response to GFs to generate neurons, astrocytes, and oligodendrocytes, and that are able to self-renew.

Self-renewal and developmental potential of RE-derived precursor cells: population analysis

Self-renewal, functional stability, and multipotency are defining attributes of stem cells. However, if the assessment of these characteristics is performed in an excessively small population compartment or for too short a time (Loeffler and Potten, 1997), transiently dividing progenitor cells may be mistaken for stem cells. To overcome this objection, we performed a long-term population analysis—for up to 6 months—on bulk cultures established from the SVZ, RE1, and RE2. At each subculturing step the total cell number was evaluated, and growth curves were generated (Gritti et al., 1999). Stem cells established from all three regions consistently expanded in number over time, displaying extended self-renewal ability (Fig. 3), although at different rates. In fact, cell lines from RE2-derived cultures grew significantly more slowly than cells from the other two regions (Fig. 3*A,B*). Of importance, no differences in the growth rate of the individual cell lines was observed at early (3–10 passages) and late stages of subculturing (18–23 passages, up to 6 months in culture) (Fig. 3*D–F*). When serially passaged cells were plated in differentiating conditions, we found that both RE1- and RE2-derived (as well as the SVZ-derived) stem-like cells always retained their ability to give rise to neurons, astrocytes, and oligodendrocytes (data not shown). Quantitative analysis of the numbers of MAP-2-, GFAP-, GalC-, and O4-IR cells as propor-

Table 2. SVZ-, RE1-, and RE2-derived stem cell progeny display stable differentiation potential

	Percentage of immunoreactive cells			
	MAP-2	GFAP	GALC	O4
Early bulk cultures (passage 7)				
SVZ	14.89 ± 5.67	54.78 ± 13.80	4.31 ± 1.97	6.92 ± 2.41
RE1	16.32 ± 4.61	60.61 ± 8.60	11.24 ± 2.39**	11.65 ± 4.67**
RE2	13.08 ± 3.80	64.23 ± 17.70	7.00 ± 1.44	6.60 ± 2.92
Late bulk cultures (passage 20)				
SVZ	15.48 ± 5.70	65.87 ± 10.97	8.21 ± 0.30	6.55 ± 1.15
RE1	16.90 ± 3.93	61.22 ± 7.52	14.07 ± 2.46**	12.47 ± 1.81**
RE2	12.92 ± 1.47	72.90 ± 5.10	6.16 ± 1.47	4.02 ± 2.02
Clonal cell lines				
B5.14 (RE1) Passage 20	12.54 ± 3.68	69.54 ± 2.75	13.66 ± 1.96	7.07 ± 1.55
A7.16 (RE2) Passage 22	10.37 ± 3.62	61.00 ± 21.00	5.63 ± 2.25	3.87 ± 3.35
Cell line from bulbectomy (A01-RE2)				
Passage 6	14.20 ± 6.30	65.37 ± 5.60	3.75 ± 0.91	6.25 ± 0.33
Passage 16	21.77 ± 3.25	53.85 ± 4.20	2.98 ± 0.85	5.95 ± 0.48

SVZ-, RE1-, and RE2-derived stem cells from early (passage 7) and late (passage 20) bulk cultures, RE1 and RE2 clonally derived stem cell lines (B5.14 and A7.16, respectively), and cell lines established from OB removed under anesthesia (A01-RE2) were allowed to differentiate by removal of GFs before processing for indirect immunofluorescence assay. The number of MAP-2-, GFAP-, GalC-, and O4-IR cells was determined in at least eight nonoverlapping fields in each sample. The total number of cells in each field was determined after counterstaining with DAPI. Data are the mean ± SD of three independent cultures, three independent experiments for each culture in which >500 cells/sample were counted in at least two samples for each experiment.

**Significantly different from SVZ and RE2, Student's t test; $p < 0.05$.

tions of the total number of cells in differentiated early cultures (passage 7) is shown in Table 2.

For cultures derived from all three regions, this ability to produce neuronal and glial cells was retained over time, and there were no appreciable differences between early and late (passage 20) cultures with regard to the numbers of neuronal and astroglial cells produced (Table 2). However, we did find significantly higher numbers of both GalC- and O4-IR cells in RE1-derived early cultures compared with SVZ- and RE2-derived cultures (Table 2, Fig. 4). Again, this property was maintained over time in culture (Table 2).

Neurotransmitter phenotype of RE stem cell-derived neuronal progeny

Previous studies have shown that SVZ stem cell-derived neuronal progeny express a specific neurotransmitter phenotype (Gritti et al., 1996). We used indirect immunofluorescence to look at CNS metabolic enzymes, neurotransmitters, and amino acids in cultures derived from RE1 and RE2, as well as SVZ. We found the presence of neuronal cells (as identified by Tuj1 positive staining) that coexpressed GABA, glutamic acid, or ChAT in both SVZ– and RE-derived cultures (Fig. 5). TH-IR cells were never observed under these differentiating conditions.

A resident population of stem cells is present along the RE

These results demonstrate that cells that exhibit multipotent stem cell features in culture are not restricted to the ventricular part of the adult SVZ–RE, but are present all along this pathway. Because the RE embodies the migration route of mitotically active neuroblasts destined for the OB, our results raise the question as to whether these stem cells derive from the migrating neuroblasts—and thus have their site of origin within the SVZ—or whether they reside in the RE itself.

To address this, we infused Ara-C onto the surface of the brain to kill actively proliferating cells (type A) in the RE, using a protocol whose effectiveness in killing off actively proliferating type A and type C cells has been previously described in the SVZ (Doetsch et al., 1999a) and recently confirmed in the hippocampus (Seri et al., 2001). Ara-C diffuses onto the brain surface, and likely this is one of the ways by which the drug exerts its antimitotic activity. Immediately after or 2 d after pump removal, EM analysis of transverse sections of the RE was performed to determine the cell type composition. Data are summarized in Table 3. After the termination of Ara-C treatment (day 0) no type A or type C cells were present in the RE. Among the cells remaining after Ara-C treatment, almost all corresponded to type B cells. A few oligodendrocytes and pyknotic cells were also detected. A small fraction of the cells could not be identified. These correspond to fragments of cells with too little cytoplasm to be classified. No cells in mitosis were present. Two days after pump removal, type C and type A cells were detectable, together with oligodendrocytes and unidentified cells. Cells in mitosis were also observed. By 14 d the proportion of the different cell types and the organization of the RE was similar to that of untreated animals (20.66% type B, 77.50% type A, scattered type C and occasional ependymal cells). These data suggest that *de novo* production of neuronal precursors after Ara-C treatment occurs in the RE with a kinetic profile similar to that previously described in the SVZ, suggesting the presence of a stem cell compartment in the RE.

To test whether neurospheres could be generated from the RE after the antimitotic treatment, RE tissue was dissected out and processed for the neurosphere-forming assay immediately after pump removal. The number of primary spheres generated in cultures derived from Ara-C-treated animals were indistinguishable from those obtained from sham-treated mice [58 ± 5 vs 51 ± 4, respectively; three separate experiments each involving three sham-treated and three Ara-C-treated animals; mean ± SD; data

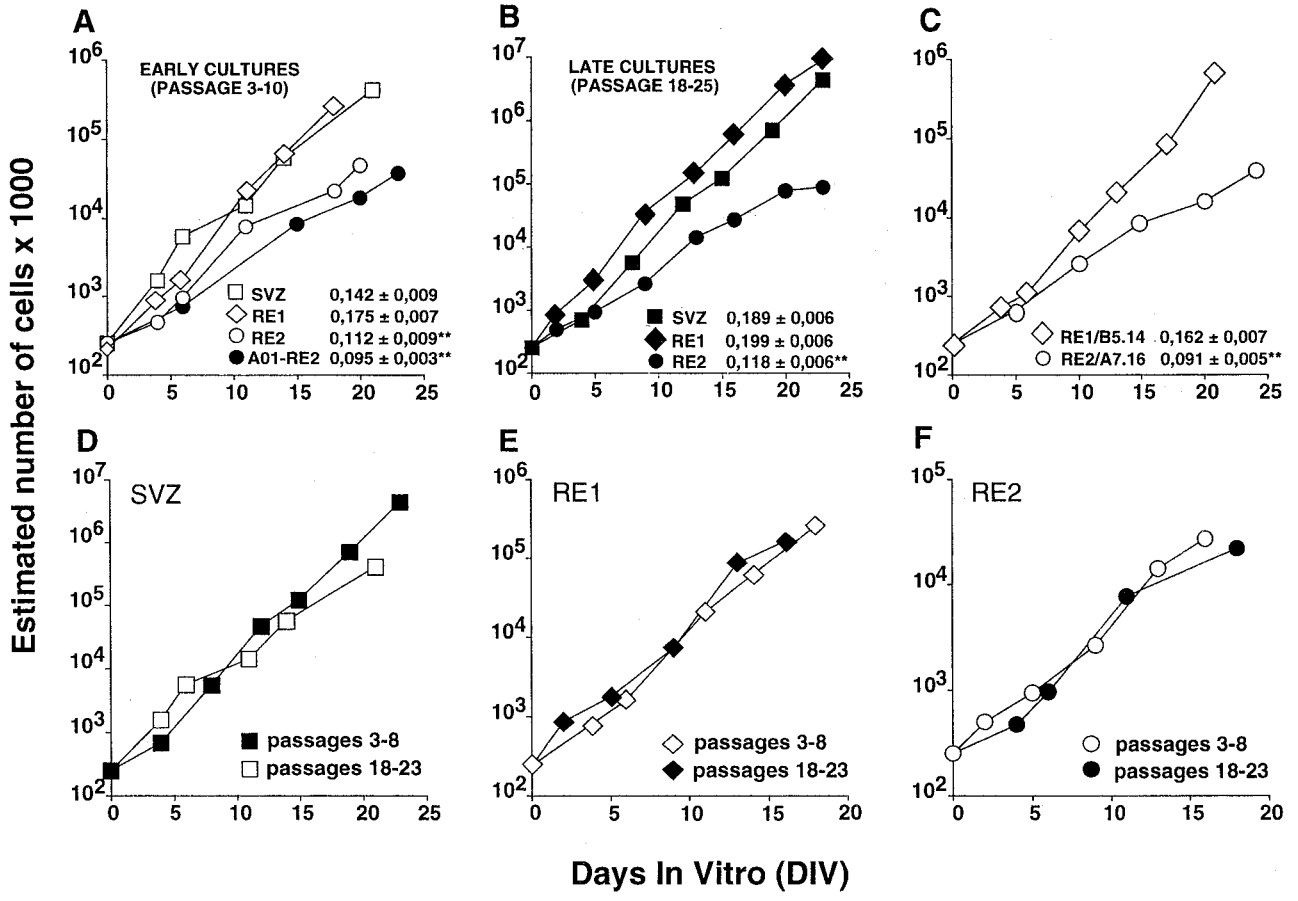

Figure 3. Stem cell lines established from the adult SVZ–RE display steady expansion rates. Cells were grown in the simultaneous presence of EGF and FGF-2, and growth curves were obtained (see Materials and Methods). Data were interpolated using a linear regression model and best fitted the following equation: $y = a + bx$, where y is the estimated total number of cells (in log scale), x is the time (DIV), a is the intercept value, and b is the slope. The values of $b \pm$ SE are shown in the *insets* in *A–C*. For *D–F*, in which the growth curves of early and late cultures from SVZ, RE1, and RE2 are compared, refer to b values shown in *A* and *B* for early and late cultures, respectively (*A, B*). The SVZ- and RE1-derived cell lines had closely similar expansion rates, whereas the rate for RE2-derived cell lines was slower, both for early (*A*) and late cultures (*B*). The expansion rates of RE1- and RE2-derived clonal cell lines (B5.14 and A7.16, respectively; *C*) and of the cell line established from surgically removed OB tissue (A01-RE2; *A*) closely matched those observed in bulk cultures established from the corresponding regions (*A, B*). Extensive subcultivation (up to 6 months *in vitro*) did not affect the growth characteristics of the SVZ- (*D*), RE1- (*E*), or RE2-derived (*F*) stem cell lines. Growth curves (early and late passages) were generated from each of three independent cultures, all of which yielded similar results. The growth curves presented are from one among the three independent cultures. The slope values were compared using a *t* test followed by a Bonferroni *post hoc* test. **Significantly different from SVZ, RE1, and RE1/B5.14; $p < 0.05$.

refer to RE2-derived cultures, although similar data were obtained with RE1 cells (data not shown)]. This shows that the SVZ-derived neuroblasts migrating in the RE are not the source of the RE-derived stem cells and further suggests that these cells reside within the RE itself.

To provide support for this conclusion, cells from the RE of untreated mice were separated into type A (migrating) and non-type A (resident) fractions (Lim and Alvarez-Buylla, 1999), and neurospheres were prepared from each fraction. Immunocytochemistry performed on cultures after dissociation showed that 77–83% of the cells in the type A fraction-derived cultures were IR to Tuj1 antibody (known to label type A precursors), and 1–2% of the cells were IR for GFAP. Conversely, in non-type A fraction-derived cultures 3–4% of the cells were Tuj1-IR, and 20–35% were GFAP-IR. When cells from each fraction were plated and subjected to neurosphere-forming assay, 128.4 ± 40.6 and 3.2 ± 0.3 spheres per well were formed in non-type A fraction- and type A fraction-derived cultures, respectively (data are the means ± SD of three separate experiments). These data show that the non-type A resident fraction is the source of neurosphere-forming stem cells in the RE.

RE-derived cell lines can be established from OB tissue obtained by unilateral olfactory bulbectomy

Unilateral olfactory bulbectomy was performed in five animals, and tissue (corresponding to the RE2 region) was cultured from each individual mouse. All the animals survived and recovered fully from surgery. Primary spheres were generated in three of the five samples (A01, A50, and A08), and bulk cultures were generated from each of them. The three cell lines showed similar growth profiles and differentiation potential; representative data from the A01 line are presented in Figure 3*A*. A01–RE2 cells proliferated and expanded in number over time, displaying extended self-renewal ability and growth rates similar to RE2-derived cultures (Fig. 3*A,B*). Indirect immunocytochemistry showed that the progeny of A01–RE2 cells generated neurons, astrocytes, and oligodendrocytes. Furthermore, the percentages

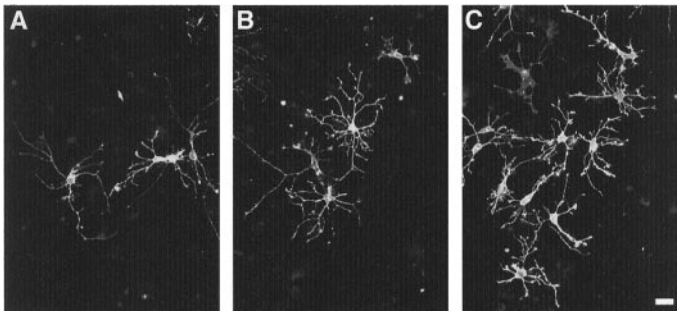

Figure 4. RE1 stem cells produce higher numbers of oligodendrocytes. SVZ-, RE1-, and RE2-derived stem cells (passages 5–23) were induced to differentiate by removal of GFs. The figure shows representative fields of stem cell-derived cultures from these regions after 6 d of differentiation and after indirect immunofluorescence with an anti-GalC antibody. Significantly less oligodendrocytes are found in SVZ (*A*) and RE2 stem cell progeny (*B*) as compared with RE1-derived cultures (*C*). See Table 2 for a detailed quantitative analysis. Scale bar, 20 μm.

of MAP-2-, GFAP-, GalC-, and O4-IR cells were similar to those found in RE2-derived cell lines (Table 2).

DISCUSSION

De novo neurogenesis has been reported in both adult rodents and higher mammalian species (Altman and Das, 1965; Das and Altman, 1971; Kaplan and Hinds, 1977; Kaplan, 1982; Rakic and Kormack, 1993). Neurogenesis occurs throughout adulthood in the SVZ of the forebrain lateral ventricles (Smart, 1961; Altman, 1969), a stem cell compartment in which new neuroblasts are generated throughout life, undergo long-distance migration along a specific migratory pathway (the RMS), and then integrate in the cortical layers of the OB (Doetsch and Alvarez-Buylla, 1996).

We provide the demonstration that multipotent, self-renewing stem cells can be isolated from the whole RE (the strip of tissue that persists after the postnatal closure of the primitive olfactory ventricle and that spans most of the OB axis), including the core of the OB.

Three lines of evidence lead to the conclusion that the RE-derived stem cells reside therein and are not derived from the SVZ-generated migrating neuroblasts, showing that the RE is not simply a conduit for the SVZ-derived neuronal progeny, but itself contains a pool of stem cells.

First, our microdissection experiments exclude the possibility that RE stem cells are derived from the parenchymal tissue surrounding the RE, because we never observed proliferation and sphere formation in cultures derived from RE-devoid tissue (Fig. 1). Second, our fractionation experiments show that neurosphere-forming cells are found only in the resident (non-type A) fraction. Third, the number of stem cells that were isolated from the RE after Ara-C treatment remained unchanged compared with control animals. After antimitotic treatment, no type A cells were detected, and the vast majority of the cells in the RE were type B cells (non-migratory cells) (Table 3). This suggests that resident type B cells are a source of RE stem cells in our cultures.

After Ara-C-induced ablation of proliferating type A cells *in vivo*, type C cells appeared within the RE (up to 14% of the total cells as compared with the barely detectable level observed in untreated animals) (Table 3). Type C cells are a hallmark of *in situ* neurogenesis (Doetsch et al., 1999b), and their appearance was accompanied by the reappearance of type A neuroblasts. This event took place 2 d after the end of the treatment (Table 3), thus the subventricular origin for these neuroblasts can be ruled out. In fact, type A cells are known to reappear in the SVZ only 4 d after the end of the antimitotic treatment (Doetsch et al., 1999b). These data show that neurogenesis occurs in the RE after Ara-C treatment. However, the contribution of *in vivo* neurogenesis in the RE under normal conditions remains unclear. There are few to no type C cells in the RE in control animals. It is conceivable that RE stem cells are quiescent but can be activated by killing off type A cells with Ara-C. Under these conditions they would be stimulated to generate type C cells similarly to what happens in the SVZ (Doetsch et al., 1999a).

Investigations on the *in vivo* derivation of neural stem cells in the adult forebrain have narrowed their sources down to SVZ

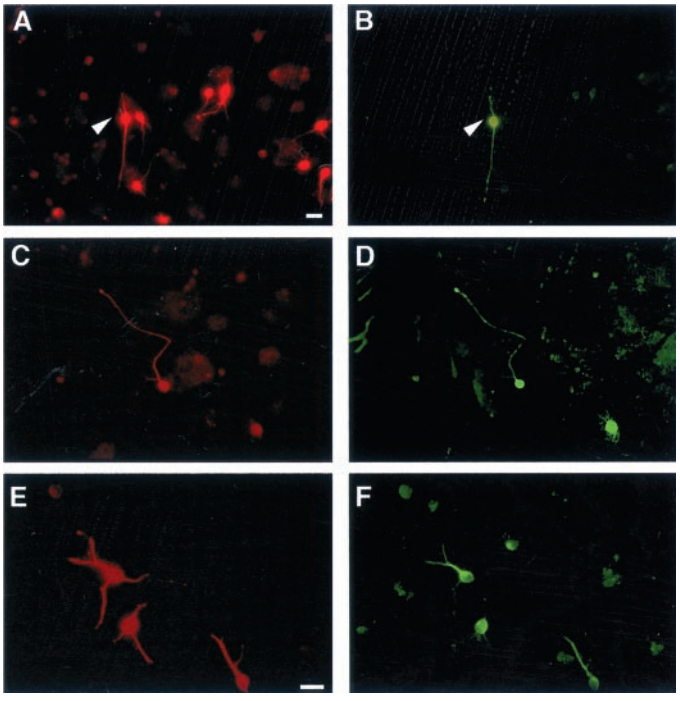

Figure 5. RE-derived stem cells generate neuronal progeny displaying different neurotransmitter phenotype. Serially passaged (passages 5–23), SVZ-, and RE-derived stem cells were allowed to differentiate for 6 d by removal of GFs. Indirect immunofluorescence revealed the presence in RE1- and RE2-derived stem cell progeny, as well as in SVZ-derived cultures, of Tuj1-IR cells (*A, C, E*) that were IR for GABA (*B*), glutamic acid (*D*), and ChAT (*F*). This figure shows representative microphotograph of RE1-derived cells. Scale bars: *A–D*, 20 μm (shown in *A*); *E*, *F*, 20 μm (shown in *E*).

Table 3. Percentages ± SE of different cell types and mitotic events at different survivals (days) after the Ara-C treatment as determined by EM analysis along rostrocaudal sections of the RE

Cell type	0 d	2 d
A	0	9.43 ± 1.94
B	92.95 ± 1.69	63.22 ± 3.62
C	0	13.89 ± 2.20
Ependymal	0	0.74 ± 0.74
Oligodendrocyte	1.32 ± 0.66	0.47 ± 0.47
Pyknotic	3.78 ± 0.22	0
Unidentified	1.95 ± 1.21	7.71 ± 0.38
Mitosis	0	3.83 ± 0.72

Data from RE1-derived sections are shown.

astrocytes (Doetsch et al., 1999a) and ependymal cells (Johansson et al., 1999). Although ependymal cells are abundant in the SVZ (20–50% of the overall cell number; Doetsch et al., 1997), this cell type is barely detectable within the RE. Given the high frequency with which stem cells are isolated from the RE of control animals and given that: (1) we never observed ciliated cells in RE cultures immediately after tissue dissociation (A. Gritti, unpublished observations); and (2) we never observed growth factor-independent proliferation of RE-derived cells (a characteristic shown by ependymal cells; Chiasson et al., 1999), we conclude that ependymal cells are unlikely to be the main source of RE stem cells in this study.

Kondo and Raff (2000) reported that when postnatal oligodendrocyte precursor cells (OPCs) are sequentially exposed to PDGF, fetal calf serum (FCS), and FGF-2, they can revert to a multipotential neural stem cell-like state. We applied our neurosphere-forming assay to tissue samples from the optic nerve of both P15 and adult mice, and in no case were we able to isolate stem cells. This shows that it is not possible to reactivate a stem cell program in OPCs using our technique. It is also important to note that: (1) the OPCs have not been described among the SVZ–RE cell types (Doetsch et al., 1997; Peretto et al., 1999); (2) our cultures are FCS-free, and we can isolate stem cells from the RE in the absence of FGF-2 or PDGF (Fig. 1); and (3) we failed to isolate stem cells from non-neurogenic regions of the forebrain devoid of RE. Altogether these data rule out the possibility that OPCs could have been the source of stem cells in our study.

Here, we used EGF and FGF-2 together to clone and propagate RE-derived neural stem cells, because the rate of expansion of these cells is much greater in the presence of both GFs than with either alone (as previously shown for SVZ stem cells) (Gritti et al., 1999). Reactivation of a latent stem-like potential after exposure to FGF-2 has been described for progenitor cells residing in non-neurogenic areas of the brain (Palmer et al., 1999). In this study, RE stem cells could always be isolated using either EGF or FGF-2 alone, whereas the number of primary spheres obtained from different regions of the SVZ–RE system remained the same, regardless of the GF combination used (Fig. 1*F*). Furthermore, we could never establish stem cell cultures from regions devoid of RE tissue under any of the conditions tested, including chronic exposure to FGF-2 (Fig. 1). Altogether, these findings indicate that RE-derived precursors do not depend on FGF-2-driven reactivation of a latent neurogenic program to display stem cell characteristics.

Interestingly, the stem cells displayed functional heterogeneity in relation to their position along the SVZ-RE axis. Whereas the proportions and of neuronal cells generated after mitogen removal were similar in each of the three SVZ–RE regions considered, the proportions of glial progeny varied. RE1-derived cultures generated more oligodendroglial cells than SVZ and the more rostral RE2 area (Table 2). Furthermore, RE2-derived cultures had a significantly slower expansion rate than the other neural stem cells, both in early and late subculturing passages. This may be attributable either to slower doubling rate or to lower frequency of symmetric division generating two stem cells (Morrison et al., 1997) compared with other SVZ–RE stem cells. Importantly, the slower expansion of RE2 cells and the greater ability of RE1 stem cells to generate oligodendroglia are intrinsic characteristics of these cells because they were retained for >6 months of *ex vivo* clonally derived culture (Table 2, Fig. 3).

It is worth noting that, although cholinergic cells are not normally observed in the OB, this phenotype is retrieved in the neuronal progeny of RE-derived stem cells. This phenomenon has been previously documented in SVZ-derived stem cell progeny (Gritti et al., 1996) and likely reflects the extreme degree of plasticity that these cells display *in vitro*.

To our knowledge, this study is the first to identify functionally distinct subsets of neural stem cells in the adult mouse forebrain. The intrinsic ability of RE1 cells to generate greater numbers of oligodendrocytes than other parts of the SVZ–RE pathway may be functionally important. After induced demyelination, oligodendrocyte precursors migrate to the corpus callosum (CC) (Nait-Oumesmar et al., 1999). It was proposed that these migrating cells originate in the SVZ and take a detour via the RE to the CC. Alternatively, they might originate from multipotent stem cells resident within the RE, which may become activated after lesioning of the CC.

The presence of multipotential stem cells throughout the RE reinforces the idea that the SVZ–RE is a neurogenic system displaying a homogeneous anatomical and histological organization (Lois and Alvarez-Buylla, 1994; Doetsch et al., 1996; Peretto et al., 1999). However, our finding that stem cells with inherently different functional characteristics occur at different levels of the adult SVZ–RE reveals a functional heterogeneity of this system. This indirectly supports previous studies from Reid et al. (1999), suggesting that different regions of the SVZ–RE pathway could give rise to specific, lineage-restricted cell types. In addition it suggests the SVZ–RE as a potential model for studying the expression, modulation, and function of key genes involved in both neural development and cell fate commitment within the adult CNS.

Neural stem cells represent a suitable source of progenitors for cell therapy in neurodegenerative disorders and brain tumors (Aboody et al., 2000). We note that the OB is easily accessible by surgery in mammals and that unilateral olfactory bulbectomy does not affect rodent survival or behavior. Moreover, bulbectomy is often performed in humans during the surgical treatment of particular brain tumors, whereas neural progenitors have been isolated from the human OB tissue (Pagano et al., 2000). We have shown that multipotential stem cell lines can be established starting from OB tissue obtained by the simple surgical procedure of unilateral olfactory bulbectomy. Once the cell line is established, the stem cell population can be expanded in long-term cultures retaining self-renewal and multipotentiality, thus providing an easily accessible source of neural cells for autologous transplantation in models of neurodegenerative diseases.

REFERENCES

Aboody KS, Brown A, Rainov NG, Bower KA, Liu S, Yang W, Small JE, Herrlinger U, Ourednik V, Black P, Breakefield XO, Snyder EY (2000) Neural stem cells display extensive tropism for pathology in adult brain: evidence from intracranial gliomas. Proc Natl Acad Sci USA 97:12846–12851.

Altman J (1969) Autoradiographic and histological studies of postnatal neurogenesis. IV. Cell proliferation and migration in the anterior forebrain, with special reference to persisting neurogenesis in the olfactory bulb. J Comp Neurol 137:433–458.

Altman J, Das GD (1965) Autoradiographic and histological evidence of postnatal hippocampal neurogenesis in rat. J Comp Neurol 124:319–335.

Chiasson BJ, Tropepe V, Morshead CM, van der Kooy D (1999) Adult mammalian forebrain ependymal and subependymal cells demonstrate proliferative potential, but only subependymal cells have neural stem cell characteristics. J Neurosci 19:4462–4472.

Craig CD, D'Sa R, Morshead CM, Roach A, van der Kooy D (1999) Migrational analysis of the constitutively proliferating subependymal population in the adult mouse forebrain. Neuroscience 93:1197–1206.

Das GD, Altman J (1971) postnatal neurogenesis in the cerebellum of the cat and tritiated thymidine autoradiography. Brain Res 30:323–330.

Doetsch F, Alvarez-Buylla A (1996) Network of tangential pathways for

neuronal migration in adult mammalian brain. Proc Natl Acad Sci USA 93:14895–14900.
Doetsch F, Garcia-Verdugo JM, Alvarez-Buylla A (1997) Cellular composition and three-dimensional organization of the subventricular germinal zone in the adult mammalian brain. J Neurosci 17:5046–5041.
Doetsch F, Caille I, Lim DA, Garcia-Verdugo JM, Alvarez-Buylla A (1999a) Subventricular zone astrocytes are neural stem cells in the adult mammalian brain. Cell 97:703–716.
Doetsch F, Garcia-Verdugo JM, Alvarez-Buylla A (1999b) Regeneration of a germinal layer in the adult mammalian brain. Proc Natl Acad Sci USA 96:11619–11624.
Gage FH (2000) Mammalian neural stem cells. Science 287:1433–1438.
Gritti A, Parati EA, Cova L, Frolichsthal P, Galli R, Wanke E, Faravelli L, Morassutti DJ, Roisen F, Nickel DD, Vescovi AL (1996) Multipotential stem cells from the adult mouse brain proliferate and self-renew in response to basic fibroblast growth factor. J Neurosci 16:1091–1100.
Gritti A, Frolichsthal P, Galli R, Parati EA, Pagano SF, Bjornson CR, Vescovi AL (1999) Epidermal and fibroblast growth factors behave as mitogenic regulators for a single, multipotent stem-like cells population from the ventricular region of the adult mouse forebrain. J Neurosci 19:3287:3297.
Johansson CB, Momma S, Clarke DL, Risling M, Lendahl U, Frisen J (1999) Identification of a neural stem cell in the adult mammalian central nervous system. Cell 96:25–34.
Kaplan MS (1982) Proliferation of subependymal cells in the adult primate CNS: differential uptake of DNA labeled precursors. J Hirnforsch 23:23–33.
Kaplan MS, Hinds JW (1977) Neurogenesis in the adult rat: electron microscope analysis of light radioautographs. Science 197:1092–1094.
Kondo T, Raff M (2000) Oligodendrocyte precursor cells reprogrammed to become multipotential CNS stem cells. Science 289:1754–1756.
Lim DA, Alvarez-Buylla A (1999) Interaction between astrocytes and adult subventricular zone precursors stimulate neurogenesis. Proc Natl Acad Sci USA 96:7526–7531.
Loeffler M, Potten CS (1997) Stem cells and cellular pedigrees - a conceptual introduction. In: Stem cells (Potten CS, ed), pp 1–27. London: Academic.
Lois C, Alvarez-Buylla A (1994) Long-distance neuronal migration in the adult mammalian brain. Science 264:1145–1148.
Lois C, Garcia-Verdugo J, Alvarez-Buylla A (1996) Chain migration of neuronal precursors. Science 271:978–981.
Luskin MB (1993) Restricted proliferation and migration of postnatally generated neurons derived from the forebrain subventricular zone. Neuron 11:173–189.
McKay R (1997) Stem cells in the central nervous system. Science 276:66–71.
Menezes JRL, Smith CM, Nelson KC, Luskin MB (1995) The division of neuronal progenitor cells during migration in the neonatal mammalian forebrain. Mol Cell Neurosci 6:496–508.
Morrison SJ, Shah NM, Anderson DJ (1997) Regulatory mechanisms in stem cell biology. Cell 88:287–298.
Morshead CM, Reynolds BA, Craig CG, McBurney MW, Staines WA, Morassutti D, Weiss S, van der Koy D (1994) Neural stem cells in the adult mammalian forebrain: a relatively quiescent subpopulation of subependymal cells. Neuron 13:1071–1082.
Nait-Oumesmar B, Decker L, Lachapelle F, Avellana-Adalid V, Bachelin C, Baron-Van Evercooren A (1999) Progenitor cells of the adult mouse subventricular zone proliferate, migrate and differentiate into oligodendrocytes after demyelination. Eur J Neurosci 11:4357–4366.
Pagano SF, Impagnatiello F, Girelli M, Cova L, Grioni E, Onofri M, Cavallaro M, Etteri S, Vitello F, Giombini S, Solero CL, Parati EA (2000) Isolation and characterization of neural stem cells from the adult human olfactory bulb. Stem Cells 18:295–300.
Palmer TD, Markakis EA, Willhoite AR, Safar F, Gage FH (1999) Fibroblast growth factor-2 activates a latent neurogenic program in neural stem cells from diverse regions of the adult CNS. J Neurosci 19:8487–8497.
Peretto P, Merighi A, Fasolo A, Bonfanti L (1999) The subependymal layer in rodents: a site of structural plasticity and cell migration in the adult mammalian brain. Brain Res Bull 49:221–243.
Rakic P, Kormack DR (1993) Constraints on neurogenesis in adult primate brain: an evolutionary advantage? In: Restorative neurology, Vol 6, Neuronal cell death and repair (Cuello AC, ed), pp 257–266. Amsterdam: Elsevier.
Reid CB, Liang I, Walsh CA (1999) Clonal mixing, clonal restriction and specification of cell types in the developing rat olfactory bulb. J Comp Neurol 403:106–118.
Reynolds BA, Weiss S (1992) Generation of neurons and astrocytes from isolated cells of the adult mammalian central nervous system. Science 255:1707–1710.
Richards KJ, Kilpatrick TJ, Bartlett PF (1992) De novo generation of neuronal cells from the adult mouse brain. Proc Natl Acad Sci USA 9:8591–8595.
Seri B, Garcia-Verdugo JM, McEwen BS, Alvarez-Buylla A (2001) Astrocytes give rise to new neurons in the adult mammalian hippocampus. J Neurosci 21:7153–7160.
Smart I (1961) The subependymal layer of the mouse brain and its cell production as shown by radioautography after thymidine-H3 injection. J Comp Neurol 116:325–338.
Stemple DL, Anderson DJ (1992) Isolation of a stem cell for neurons and glia of the mammalian neural crest. Cell 71:1–20.
Temple S, Alvarez-Buylla A (1999) Stem cells in the adult mammalian central nervous system. Curr Opin Neurobiol 9:135–141.
Weiss S, Reynolds BA, Vescovi AL, Morshead C, Craig CG, van der Kooy D (1996) Is there a neural stem cell in the mammalian forebrain? Trends Neurosci 19:387–393.
Wichterle H, Garcia-Verdugo JM, Alvarez-Buylla A (1997) Direct evidence for homotypic, glia-independent neuronal migration. Neuron 18:779–791.